ARL
The University of Texas at Austin

TECHNICAL REPORT

14 March 2002
ARL-TR-02-03

Copy Number 8

Estimation of Receiver Operating Characteristic Curves for Multiping Mine Detection Using Empirical Target Data

Technical Report under Contract N00039-96-D-0051, TO No. 0329
TD No. 2506054, Multiple-Ping Processing for Detection of Targets on the Sea Bottom

Petre I. Rusu and S. Patrick Pitt

Prepared for: Office of Naval Research, Code 32MIW
Department of the Navy • Arlington, VA 22217-5660

Monitored by: Naval Sea Systems Command
Department of the Navy • Washington, DC 20362-5101

Acknowledgment of Support and Disclaimer (May 1995) (DFARS 252.235-7010) as required by Contract N00039-96-D-0051: This material is based upon work supported by the Naval Sea Systems Command under Contract No. N00039-96-D-0051, Task Order No. *0329*. Any opinions, findings and conclusions, or recommendations expressed in this material are those of the author(s) and do not necessarily reflect the views of the Naval Sea Systems Command.

Approved for public release; distribution is unlimited.

Applied Research Laboratories • The University of Texas at Austin • Post Office Box 8029 • Austin, Texas 78713-8029

REPORT DOCUMENTATION PAGE

Form Approved
OMB No. 0704-0188

1. REPORT DATE *(DD-MM-YYYY)*	2. REPORT TYPE	3. DATES COVERED *(From - To)*
14-03-2002	technical	

4. TITLE AND SUBTITLE
Estimation of Receiver Operating Characteristic Curves for Multiping Mine Detection Using Empirical Target Data
Technical Report under Contract N00039-96-D-0051, TO No. 0329, TD No. 2506054, Multiple-Ping Processing for Detection of Targets on the Sea Bottom

5a. CONTRACT NUMBER
N00039-96-D-0051

5b. GRANT NUMBER
NA

5c. PROGRAM ELEMENT NUMBER
0602315N

6. AUTHOR(S)
Rusu, Petre I., and Pitt, S. Patrick

5d. PROJECT NUMBER
TO No. 0329

5e. TASK NUMBER
TD No. 2506054

5f. WORK UNIT NUMBER
NA

7. PERFORMING ORGANIZATION NAME(S) AND ADDRESS(ES)
Applied Research Laboratories
The University of Texas at Austin
P.O. Box 8029
Austin, TX 78713-8029

8. PERFORMING ORGANIZATION REPORT NUMBER
ARL-TR-02-03

9. SPONSORING/MONITORING AGENCY NAME(S) AND ADDRESS(ES)
Office of Naval Research
Department of the Navy
Arlington, VA 22217-5660

Naval Sea Systems Command
Department of the Navy
Washington, DC 20362-5101

10. SPONSOR/MONITOR'S ACRONYM(S)
ONR / NAVSEA

11. SPONSORING/MONITORING AGENCY REPORT NUMBER

12. DISTRIBUTION AVAILABILITY STATEMENT
Approved for public release; distribution is unlimited.

13. SUPPLEMENTARY NOTES
Acknowledgment of Support and Disclaimer (May 1995) (DFARS 252.235-7010) as required by Contract N00039-96-D-0051: This material is based upon work supported by the Naval Sea . . . (cont'd on reverse side)

14. ABSTRACT
This report develops the formalism for computing receiver operating characteristic (ROC) curves for an active sonar detector, consisting of linear receiver processing followed by a linear envelope detector. The formalism is applicable to both single-ping and multiple-ping detection. The methodology for computing the ROC curves directly incorporates measurements of target strength as a function of aspect angle to estimate the requisite signal-plus-noise probability density function (pdf) under the assumption of Gaussian background statistics. This "empirical" approach for computing the probability of detection allows ROC curve performance to be estimated for multiple ping integration and for any sensor–target scenario that is supported by the available target data.

15. SUBJECT TERMS
angle target detection; multiping; receiver operating characteristics; ROC; target aspect; target strength measurements

16. SECURITY CLASSIFICATION OF:			17. LIMITATION OF ABSTRACT	18. NUMBER OF PAGES	19a. NAME OF RESPONSIBLE PERSON
a. REPORT	b. ABSTRACT	c. THIS PAGE			S. Patrick Pitt
U	U	U	NA	30	19b. TELEPHONE NUMBER *(Include area code)* 512/835-3513

11. SUPPLEMENTARY NOTES (cont'd)

Acknowledgment of Support and Disclaimer (May 1995) (DFARS 252.235-7010) (cont'd)

Systems Command under Contract No. N00039-96-D-0051, Task Order No. 0329. Any opinions, findings and conclusions, or recommendations expressed in this material are those of the author(s) and do not necessarily reflect the views of the Naval Sea Systems Command.

TABLE OF CONTENTS

This page intentionally left blank.

LIST OF FIGURES

Figure **Page**

This page intentionally left blank.

ACKNOWLEDGMENT

The authors are indebted to Dr. Kent Scarbrough for his careful review and suggestions, verification of results, and assistance in the final editing of this report.

This page intentionally left blank.

1. INTRODUCTION

This work is a contribution to the solution of the performance prediction problem for multiping detectors of target echoes. The formalism presented here applies to a typical active sonar detection problem. Echoes resulting from pulsed transmit waveforms are input to a predetection stage (matched filter), followed by a linear detector and a postdetection integrator.

Specifically, we wish to characterize the expected detection performance for an encounter with a real target, including the dependence of target strength on the observed target aspect – that is, the dependence of the signal amplitude of the received echo on the target aspect. We present an approach for the generation of receiver operating characteristic (ROC) curves for a linear detector operating on signals in Gaussian noise, where the signal amplitude statistics are determined from empirical target strength data.

The results are a practical extension of some rather old results in detection theory. Originally, Marcum[1,2] solved the detection problem for the case of a sinusoidal (constant amplitude) signal in Gaussian noise. Marcum's results were extended by Swerling,[3,4] Kaplan,[5] Schwartz,[6] and others to fluctuating signals, where the fluctuations were described by analytic densities that made it possible to find approximate closed-form solutions for the multivariate densities of interest. These cases were reduced by Swerling, in work performed prior to 1966 but only published 30 years later,[7] to particular cases of the generalized chi-square distribution. In the same work, he discussed the possibility of using chi-square density functions to fit cases usually modeled with log-normal density functions.

These prior studies[1–7] were performed in the context of radar physics. The empirical data that motivated many of these studies consisted of observations of target cross section as a function of aspect angle. In each case the empirical probability density function (pdf) of the measured data was approximated with an analytic pdf. This analytic pdf was then used to develop a solution to the performance estimation problem.

The methods developed in this work use target strength measurements from a target of interest as an empirical estimate of the signal pdf at the linear detector output. This empirical pdf is then used in the computation of single-ping and multiping detector ROC curves for the target of interest. The detection statistic is the envelope amplitude (or sum of envelope amplitudes) at the linear detector output. The random value taken by the detection statistic depends on the target aspect angle, the transmit pulse duration and bandwidth, and the statistical characteristics of the additive noise.

The problem is to decide whether a target is present or absent, based on the value of a univariate random variable, the detection statistic. Denoting the "target present"

hypothesis by H_1, and the "noise only" hypothesis by H_0, the detection statistic $\hat{z}$ is described by the pdf $p_0(z)$ if H_0 is true, and by $p_1(z)$, if H_1 is true. To simplify the notation, the signal-to-noise ratio (SNR) dependence is omitted. The detection statistic is compared to a threshold value, b, that divides the range of values for $\hat{z}$ into two regions, $R_0 = \{z \leq b\}$ and $R_1 = \{z > b\}$. The decision rule is to decide that H_0 is true if $z \in R_0$, and H_1 is true if $z \in R_1$.

Detector performance is typically described by the relation between the probability of detection, P_d, and the probability of false alarm, P_{fa}, for specified values of the SNR at the linear detector input. P_d represents the probability that the detection statistic is larger than a threshold value when both signal and noise are present. P_{fa} is the probability that the detection statistic is larger than the threshold when only noise is present. The probability of detection is given by

$$P_d = \int_b^\infty p_1(z)\, dz \ , \tag{1.1}$$

and the probability of false alarm by

$$P_{fa} = \int_b^\infty p_0(z)\, dz \ . \tag{1.2}$$

Together Eqs. (1.1) and (1.2) represent the parametric form of the receiver operating characteristic curve. Implicit and explicit nonparametric forms, $F(P_{fa}, P_d) = 0$ and $P_d = P_d(P_{fa})$, can be obtained by eliminating the threshold b between (1.1) and (1.2).

The formalism developed here applies to both single-ping and multiping detection processes. In the multiping case, the intermediate observation vector, $\mathbf{x}$, is made up of the linear detector outputs from successive echoes, and represents an observed value of a multivariate random variable $\hat{\mathbf{x}}$. The postdetection integrator sums or averages the detector outputs from successive echoes to generate a scalar quantity, z, on which the final decision is based. Thus, the multivariate random variable $\hat{\mathbf{x}}$ is mapped into a univariate detection statistic $\hat{z}$.

The empirical data used to represent the signal amplitude at the linear detector output consists of peak target strength measurements from underwater targets of various sizes and shapes. The target strength measurements quantify the reflectivity of a particular target as a function of the target aspect angle relative to the transmitter and receiver. These measurements were performed in a controlled environment essentially free of noise. The aggregate noise at the detector input (external reverberation, receiver noise, etc.) is assumed to be zero-mean, Gaussian, and uncorrelated from one echo to the next. Thus, the noise amplitude has a Rayleigh density at the linear detector output.

The development in the following sections makes extensive use of the Rayleigh and Rice (or Rayleigh-Rice) density functions. The Rayleigh pdf is given by

$$\rho(x,\sigma) = \frac{x}{\sigma^2}\ \exp\Big(-\frac{x^2}{2\sigma^2}\Big)\ , \tag{1.3}$$

and the Rice pdf is

$$R(r,s,\sigma) = \frac{r}{\sigma^2}\ \exp\Big(-\frac{r^2+s^2}{2\sigma^2}\Big)\ I_0\Big(\frac{rs}{\sigma^2}\Big)\ . \tag{1.4}$$

The rest of this report is organized as follows. Section 2 develops the methodology for computing ROC curves based on empirical target strength data for the single-ping case. Although all of the results presented in Section 2 can be obtained as particular forms of the more general multiping results, it is convenient to first work out the simpler single-ping case. Section 3 then derives the corresponding ROC curve equations for the multiping case. Section 4 presents selected numerical results obtained with a MATLAB implementation of the analytical methodology. These results demonstrate the capability to provide an accurate quantitative description of performance for the class of linear detectors and for specific targets of interest.

This page intentionally left blank.

2. SINGLE-PING ROC CURVE ESTIMATION

2.1 THE GENERAL CASE

The target strength (signal amplitude) is denoted in what follows by s and the corresponding random variable (RV) by $\hat{s}$. The target aspect angle dependence, the source of the variations in the signal amplitude, is implicit. The detection problem for a given aspect angle is equivalent to the detection of a sinusoidal signal of amplitude s and phase θ. It is assumed here that the associated univariates $\hat{s}$ and $\hat{\theta}$ are independent RVs distributed on $[0,\infty)$ and $[0,2\pi)$, respectively. The density functions for $\hat{s}$ and $\hat{\theta}$ are respectively $f_{\hat{s}}(r)$ and $f_{\hat{\theta}}(\theta)$. The joint pdf for $(\hat{s},\hat{\theta})$ is therefore given by

$$f_{\hat{s}\hat{\theta}}(s,\theta) = f_{\hat{s}}(s)\ f_{\hat{\theta}}(\theta)\ . \tag{2.1}$$

If we form the new RV

$$\hat{\mathbf{s}} = (\hat{x},\hat{y}) = \hat{s}\mathrm{e}^{i\hat{\theta}} = (\hat{s}\cos\hat{\theta}, \hat{s}\sin\hat{\theta})\ , \tag{2.2}$$

the pdfs for $(\hat{x},\hat{y})$ and $(\hat{s},\hat{\theta})$ are related by

$$f_{\hat{x}\hat{y}}(x,y) = \frac{1}{s} f_{\hat{s}\hat{\theta}}(s,\theta) = \frac{1}{s} f_{\hat{s}}(s) f_{\hat{\theta}}(\theta)\ , \tag{2.3}$$

where $(x,y) = (s\cos\theta, s\sin\theta)$.

Similarly, the noise is denoted by amplitude n and phase ϕ. The corresponding RVs, $\hat{n}$ and $\hat{\phi}$, are distributed on $[0,\infty)$ and $[0,2\pi)$ and are assumed to be independent, with pdfs $f_{\hat{n}}(n)$ and $f_{\hat{\phi}}(\phi)$. The joint pdf for (n,ϕ) is

$$f_{\hat{n}\hat{\phi}}(n,\phi) = f_{\hat{n}}(n)\ f_{\hat{\phi}}(\phi)\ . \tag{2.4}$$

The new RV

$$\hat{\mathbf{n}} = (\hat{u},\hat{v}) = \hat{n}\ \mathrm{e}^{i\hat{\phi}} \tag{2.5}$$

will then have the density

$$f_{\hat{u}\hat{v}}(u,v) = \frac{1}{n}\, f_{\hat{n}\hat{\phi}}(n,\phi) = \frac{1}{n}\, f_{\hat{n}}(n)\ f_{\hat{\phi}}(\phi)\ . \tag{2.6}$$

It is assumed that $\hat{s}$, $\hat{\theta}$, $\hat{n}$, and $\hat{\phi}$ are mutually independent random variables. This implies that $\hat{\mathbf{s}}$ and $\hat{\mathbf{n}}$ are independent, and, consequently, the pdf of $\hat{\mathbf{s}}+\hat{\mathbf{n}}$ is given by the convolution of the pdfs of $\hat{\mathbf{s}}$ and $\hat{\mathbf{n}}$,

$$f_{\hat{\mathbf{s}}+\hat{\mathbf{n}}} = f_{\hat{\mathbf{s}}} * f_{\hat{\mathbf{n}}}. \tag{2.7}$$

For the single-ping detection case, the probability of detection and probability of false alarm, (1.1) and (1.2), are given by

$$P_d(b) = \int_b^\infty f_{|\hat{\mathbf{s}}+\hat{\mathbf{n}}|}(r)\ dr \tag{2.8}$$

and

$$P_{fa}(b) = \int_b^\infty f_{|\hat{\mathbf{n}}|}(r)\ dr\ . \tag{2.9}$$

The values of P_d and P_{fa} in (2.8) and (2.9) define a point on the ROC curve for any common value of the threshold, b, corresponding to a specified SNR value, γ, where

$$\gamma = \frac{\mathrm{E}\{s^2\}}{2\sigma^2}\ . \tag{2.10}$$

The problem is to express $f_{|\hat{\mathbf{s}}+\hat{\mathbf{n}}|}$ in terms of the known pdfs $f_{\hat{s}}(s)$, $f_{\hat{\theta}}(\theta)$, $f_{\hat{n}}(n)$, and $f_{\hat{\phi}}(\phi)$.

It is assumed here that the phases θ and ϕ are uniformly distributed on $[0, 2\pi)$ so that

$$f_{\hat{\theta}}(\theta) = f_{\hat{\phi}}(\phi) = \frac{1}{2\pi}\ . \tag{2.11}$$

Further, it is assumed that $\hat{\mathbf{n}}$ is normally distributed and that each of its components, $\hat{u}$ and $\hat{v}$, is zero-mean and has a standard deviation equal to σ. This implies that $\hat{n} = |\hat{\mathbf{n}}|$ is distributed according to the Rayleigh pdf

$$f_{\hat{n}}(n) = \rho(n, \sigma)\ . \tag{2.12}$$

One may note that since $\hat{n}$ and $\hat{\phi}$ are statistically independent, $\hat{u}$ and $\hat{v}$ are uncorrelated and zero-mean. Given that the RVs $\hat{u}$ and $\hat{v}$ are Gaussian and uncorrelated, it follows that they are also statistically independent.

The signal-plus-noise density function of (2.7) can be written as a convolution integral,

$$f_{\hat{\mathbf{s}}+\hat{\mathbf{n}}}(x, y) = \int_{-\infty}^{\infty} dx' \int_{-\infty}^{\infty} dy'\ f_{\hat{\mathbf{s}}}(x', y')\ f_{\hat{\mathbf{n}}}(x - x', y - y')\ . \tag{2.13}$$

Changing the original integration variables to polar coordinates according to $(x', y') = (r' \cos\theta', r' \sin\theta')$ allows the right-hand side of (2.13) to be written in terms of $f_{\hat{s}}$ and $f_{\hat{n}}$. Similarly, it is convenient to express the independent variables in polar coordinates as $(x, y) = (r \cos\theta, r \sin\theta)$. With this change of variables (2.13) becomes

$$\begin{aligned} &f_{\hat{\mathbf{s}}+\hat{\mathbf{n}}}(r\cos\theta, r\sin\theta) \\ &= \int_0^\infty dr'\ r' \int_0^{2\pi} d\theta'\ f_{\hat{x}\hat{y}}(r'\cos\theta', r'\sin\theta')\ f_{\hat{u}\hat{v}}(r\cos\theta - r'\cos\theta',\ r\sin\theta - r'\sin\theta'). \end{aligned} \tag{2.14}$$

Using (2.3) and (2.6), (2.14) can be written as

$$\begin{aligned} f_{\hat{\mathbf{s}}+\hat{\mathbf{n}}}(r\cos\theta, r\sin\theta) = \int_0^\infty dr' \int_0^{2\pi} d\theta' f_{\hat{s}}(r') f_{\hat{\theta}}(\theta') \\ \left[\frac{f_{\hat{n}}(\sqrt{r^2 + r'^2 - 2rr'\cos(\theta' - \theta)})}{\sqrt{r^2 + r'^2 - 2rr'\cos(\theta' - \theta)}} f_{\hat{\phi}}\Big(\tan^{-1}\big(\frac{r\sin\theta - r'\sin\theta'}{r\cos\theta - r'\cos\theta'}\big)\Big)\right]. \end{aligned} \tag{2.15}$$

Then applying the uniform phase assumption (2.11) to (2.15) leads to

$$f_{\hat{\mathbf{s}}+\hat{\mathbf{n}}}(r\cos\theta, r\sin\theta) = \frac{1}{4\pi^2}\int_0^\infty dr' f_{\hat{s}}(r')\int_0^{2\pi} d\theta' \frac{f_{\hat{n}}(\sqrt{r^2+r'^2-2rr'\cos(\theta'-\theta)})}{\sqrt{r^2+r'^2-2rr'\cos(\theta'-\theta)}} . \tag{2.16}$$

If the noise amplitude is described by the Rayleigh distribution, the introduction of (1.3) into (2.16) yields

$$f_{\hat{\mathbf{s}}+\hat{\mathbf{n}}}(r\cos\theta, r\sin\theta) = \frac{1}{2\pi\sigma^2}\mathrm{e}^{-\frac{r^2}{2\sigma^2}} g\int_0^\infty d'r\ f_{\hat{s}}(r')\ \mathrm{e}^{-\frac{r'^2}{2\sigma^2}}\ \frac{1}{2\pi}\int_0^{2\pi} d\theta'\ \mathrm{e}^{\frac{rr'\cos(\theta'-\theta)}{\sigma^2}} . \tag{2.17}$$

The appearance of the Bessel function

$$I_0(x) = J_0(ix) = \frac{1}{2\pi}\int_0^{2\pi} \mathrm{e}^{x\cos(\theta-\theta')}d\theta \tag{2.18}$$

in (2.17) makes it possible to rewrite this expression in terms of the Rice pdf, defined in (1.4), as

$$f_{\hat{\mathbf{s}}+\hat{\mathbf{n}}}(r\cos\theta, r\sin\theta) = \frac{1}{2\pi r}\int_0^\infty ds\ f_{\hat{s}}(s)\ R(r,s,\sigma) . \tag{2.19}$$

Notice that $f_{\hat{\mathbf{s}}+\hat{\mathbf{n}}}$ is normalized because $f_{\hat{s}}$ and $R(\cdot,s,\sigma)$ have unit area.

From (2.19) one can see that the density of $\hat{\mathbf{s}}+\hat{\mathbf{n}}$ in polar coordinates does not depend on the phase. This implies that the RVs $|\hat{\mathbf{s}}+\hat{\mathbf{n}}|$ and $\arg(\hat{\mathbf{s}}+\hat{\mathbf{n}})$ are independent and that $f_{\arg(\hat{\mathbf{s}}+\hat{\mathbf{n}})}(\theta) = \frac{1}{2\pi}$. From

$$f_{\hat{\mathbf{s}}+\hat{\mathbf{n}}}(r\cos\theta, r\sin\theta) = \frac{1}{2\pi r} f_{|\hat{\mathbf{s}}+\hat{\mathbf{n}}|}(r) \tag{2.20}$$

and from (2.19), it follows that

$$f_{|\hat{\mathbf{s}}+\hat{\mathbf{n}}|}(r) = \int_0^\infty ds\ f_{\hat{s}}(s)\ R(r,s,\sigma) . \tag{2.21}$$

That is, the unconditional density function $f_{|\hat{\mathbf{s}}+\hat{\mathbf{n}}|}$ is the expected value of a conditional density function, namely the Rice function $R(r,s,\sigma)$, where $R(r,s,\sigma)$ is dependent on the constrained signal amplitude, s, with univariate pdf $f_{\hat{s}}(s)$.

One may note that (2.21) can be expressed in terms of the Hankel transform defined by

$$[\mathcal{H}_0 f](r) = \int_0^\infty ds\ s\, f(r)\, J_0(rs) . \tag{2.22}$$

Taking into account that $I_0(x) = J_0(ix)$, (2.21) can be written as

$$f_{|\hat{\mathbf{s}}+\hat{\mathbf{n}}|}(r) = \frac{r}{\sigma^2}\ \mathrm{e}^{-\frac{r^2}{2\sigma^2}}\ \mathcal{H}_0\Big\{\frac{f_{\hat{s}}(s)}{s}\ \mathrm{e}^{-\frac{s^2}{2\sigma^2}}\Big\}\Big(\frac{-ir}{\sigma^2}\Big) . \tag{2.23}$$

Using this formulation, the signal-plus-noise density may be computed numerically via a 2-D Fourier transform, a frequency domain method for computing the 1-D Hankel transform.[8,10]

The probability of detection is obtained by introducing (2.21) in (2.8) and evaluating the threshold-dependent integral,

$$P_d(b) = \int_0^\infty ds\ f_{\hat{s}}(s) \int_b^\infty dr\ R(r,s,\sigma)\ . \tag{2.24}$$

Since the noise amplitude is assumed to be Rayleigh distributed, the probability of false alarm can be expressed with a simple analytic formula. Introducing (1.3) in (2.9), the probability of false alarm is given by

$$P_{fa}(b) = \int_b^\infty ds\ \frac{s}{\sigma^2} \exp\Big(-\frac{s^2}{2\sigma^2}\Big) = \exp\Big(-\frac{b^2}{2\sigma^2}\Big)\ . \tag{2.25}$$

Solving (2.25) for b and substituting into (2.24) gives

$$P_d(P_{fa},\sigma) = \int_0^\infty ds\ f_{\hat{s}}(s) \int_{2\sigma^2 \ln \frac{1}{P_{fa}}}^\infty dr\ R(r,s,\sigma)\ . \tag{2.26}$$

The ROC curve can be represented graphically as a set of points in the plane with coordinates $(x,y) = (P_{fa}(b), P_d(b))$ by giving the threshold parameter b a set of convenient values.

The empirical estimate of the signal probability density function, $f_{\hat{s}}(s)$, is defined as

$$f_{\hat{s}}^E(s) = \frac{1}{N} \sum_{i=1}^N \delta(s - s_i)\ , \tag{2.27}$$

where $\{s_i\}_{i=1}^N$ is the set of target strength observations at N equally likely values of the aspect angle. The empirical estimate for the probability of detection follows by replacing the probability density function in (2.26) with its empirical estimate (2.27). The empirical estimate of P_d is then obtained as

$$P_d^E(P_{fa},\sigma) = \frac{1}{N} \sum_{i=1}^N P_d^R(P_{fa}, s_i, \sigma)\ , \tag{2.28}$$

where

$$P_d^R(P_{fa},s,\sigma) = \int_{2\sigma^2 \ln \frac{1}{P_{fa}}}^\infty dr\ R(r,s,\sigma)\ , \tag{2.29}$$

and where P_{fa} is given by (2.25). Thus, the P_d for any given aspect angle can be computed by numerically integrating (2.29), and the P_d over all aspect angles (the expected value of P_d when the aspect angle is unknown) is computed from (2.28).

2.2 SPECIAL CASES

Any special case that has an analytic solution is useful for checking the numerical implementation of the theoretical results. Two such special cases, the constant amplitude signal and the Rayleigh-fading signal, are considered below.

2.2.1 Constant Amplitude Signal

Expression (2.21) takes a simpler form for a constant amplitude sinusoidal signal, in which case the pdf of the signal amplitude is a Dirac delta function,

$$f_{\hat{s}}(r) = \delta(r - r_0) \ . \tag{2.30}$$

From (2.21) it follows at once that

$$f_{|\hat{\mathbf{s}}+\hat{\mathbf{n}}|}(r) = R(r, r_0, \sigma) \ , \tag{2.31}$$

which shows the well-known fact that the pdf of the linear detector output for a sinusoidal signal in Gaussian noise is given by the Rayleigh-Rice function, as defined by (1.4). ROC curves for this case have been estimated and published by Robertson.[11]

2.2.2 Rayleigh Distributed Signal

Consider the case where both the signal and noise amplitudes are Rayleigh distributed at the linear detector output. The signal and noise pdfs are given by

$$f_{\hat{s}}(s) = \rho(s, \mu) \quad \text{and} \quad f_{\hat{n}}(n) = \rho(n, \sigma) \ , \tag{2.32}$$

where μ and σ are the Rayleigh parameters.

Now (2.21) can be put in a simple form with the help of the following relationship [9, eq. 11.4.29, p. 486]:

$$\int_0^\infty \mathrm{e}^{-a^2t^2} t^{\nu+1} J_\nu(bt)\, dt = \frac{b^\nu}{(2a^2)^{\nu+1}} \mathrm{e}^{-\frac{b^2}{4a^2}} \qquad (\Re\nu > -1, \quad \Re a^2 > 0) \ . \tag{2.33}$$

Let $\nu = 0$, $a^2 = \frac{\sigma^2+\mu^2}{2\sigma^2\mu^2}$, and $b = i\frac{r}{\sigma^2}$ in (2.33); then one can write (2.21) as

$$f_{|\hat{\mathbf{s}}+\hat{\mathbf{n}}|}(r) = \frac{r}{\sigma^2 + \mu^2} \mathrm{e}^{-\frac{r^2}{2(\sigma^2+\mu^2)}} \ . \tag{2.34}$$

This follows from the fact that the sum of two independent Gaussian RVs is also a Gaussian RV.

Substituting (2.34) into (2.8), it follows directly that P_d is given by

$$P_d(b) = \exp\Big(-\frac{1}{2}\frac{b^2}{\sigma^2 + \mu^2}\Big) \ . \tag{2.35}$$

The threshold b can be easily eliminated between (2.25) and (2.35) to obtain the analytic relation between P_d, P_{fa}, and γ as

$$P_d = P_{fa}^{\ \frac{1}{1+\gamma}} \ , \tag{2.36}$$

where $\gamma = \mu/\sigma$.

This page intentionally left blank.

3. MULTIPING ROC CURVE ESTIMATION

3.1 THE GENERAL CASE

We now consider a processor that sums M independent samples at the output of the linear detector. In particular, we consider the multiping processor where the M samples represent the peak linear detector output from M successive echoes. The signal and noise components at the linear detector output for the i-th echo are

$$\mathbf{n}_i = (n_{ix}, n_{iy}) = (n_i \cos(\psi_i), n_i \sin(\psi_i)), \tag{3.1}$$

and

$$\mathbf{s}_i = (s_{ix}, s_{iy}) = (s_i \cos(\phi_i), s_i \sin(\phi_i)). \tag{3.2}$$

Each observation of the multivariate signal RV consists of M scalar observations $(\hat{s}_1, \ldots, \hat{s}_M)$. The ensemble of these observations form the set $\{(s_{1k}, \ldots, s_{Mk})\}_{k=1}^{N}$. Introducing the notation

$$\mathbf{v}_i = \mathbf{s}_i + \mathbf{n}_i \ , \tag{3.3}$$

the detection statistic is given by

$$\hat{z} = \sum_{i=1}^{M} \hat{v}_i = \sum_{i=1}^{M} |\hat{\mathbf{s}}_i + \hat{\mathbf{n}}_i| \tag{3.4}$$

when the target is present, and by

$$\hat{z} = \sum_{i=1}^{M} \hat{n}_i = \sum_{i=1}^{M} |\hat{\mathbf{n}}_i| \tag{3.5}$$

when only noise is present. The P_d and P_{fa} for a given threshold b are then

$$P_d(b) = \int_b^{\infty} f_{\hat{v}_1 + \cdots + \hat{v}_M}(r) \ dr \tag{3.6}$$

and

$$P_{fa}(b) = \int_b^{\infty} f_{\hat{n}_1 + \cdots + \hat{n}_M}(r) \ dr \ . \tag{3.7}$$

The SNR of an individual echo (ping i, aspect k) is defined by

$$\gamma_{ik} = \frac{s_{ik}^2}{2\sigma^2} \ , \tag{3.8}$$

and the average SNR over all aspects for a given ping index, i, is

$$\gamma_i = \frac{1}{N} \sum_{k=1}^{N} \gamma_{ik}. \tag{3.9}$$

Here we only consider those detection scenarios where the noise statistics do not change from ping to ping.

As in the 1-D (single-ping) case, it is assumed that the angular parts of $\mathbf{s}_i$ and $\mathbf{n}_i$ are independent of the radial parts, independent of each other, and are uniformly distributed on $[0, 2\pi)$. This implies that

$$f_{\mathbf{s}_i}(x_i, y_i) = \frac{1}{s_i} f_{\hat{s}_i \hat{\phi}_i}(s_i, \phi_i) = \frac{1}{s_i} f_{\hat{s}_i}(s_i) f_{\hat{\phi}}(\phi_i) \ , \tag{3.10}$$

with $s_i = |\mathbf{s}_i| = \sqrt{s_{ix} + s_{iy}}$ and $\phi_i = \arctan \frac{s_{iy}}{s_{ix}}$, and

$$f_{\hat{n}_i \hat{\psi}_i}(x_i, y_i) = \frac{1}{n_i} f_{\hat{n}_i \hat{\psi}_i}(n_i, \psi_i) = \frac{1}{n_i} f_{\hat{n}_i}(r) f_{\hat{\psi}}(\psi_i) \ , \tag{3.11}$$

with $n_i = \sqrt{n_{ix} + n_{iy}}$ and $\psi_i = \arctan \frac{n_{iy}}{n_{iy}}$. The mutual independence of the radial and angular components and the uniform distribution of the phase component on $[0, 2\pi)$, for both the signal and noise, allow one to write

$$\begin{aligned} f_{\hat{\mathbf{s}}_1 \hat{\mathbf{s}}_2 \ldots \hat{\mathbf{s}}_M}(\hat{\mathbf{s}}_1, \hat{\mathbf{s}}_2, \ldots, \hat{\mathbf{s}}_M) &= f_{\hat{s}_{1x} \hat{s}_{1y} \hat{s}_{2x} \hat{s}_{2y} \ldots \hat{s}_{Mx} \hat{s}_{My}}(s_{1x}, s_{1y}, s_{2x}, s_{2y}, \ldots, s_{Mx}, s_{My}) \\ &= \Big(\prod_{i=1}^{M} \frac{1}{s_i}\Big) f_{\hat{s}_1 \hat{s}_2 \ldots \hat{s}_M}(s_1, s_2, \ldots s_M) \cdot f_{\hat{\phi}_1 \hat{\phi}_2 \ldots \hat{\phi}_M}(\phi_1, \phi_2, \ldots, \phi_M) \\ &= \Big(\frac{1}{2\pi}\Big)^M \Big(\prod_{i=1}^{M} \frac{1}{s_i}\Big) f_{\hat{s}_1 \hat{s}_2 \ldots \hat{s}_M}(s_1, s_2, \ldots, s_M) \ , \end{aligned} \tag{3.12}$$

and

$$\begin{aligned} f_{\hat{\mathbf{n}}_1 \hat{\mathbf{n}}_2 \ldots \hat{\mathbf{n}}_M}(\mathbf{n}_1, \mathbf{n}_2, \ldots, \mathbf{n}_M) &= f_{\hat{\mathbf{n}}_1}(\mathbf{n}_1)\ f_{\hat{\mathbf{n}}_2}(\mathbf{n}_2) \cdots f_{\hat{\mathbf{n}}_M}(\mathbf{n}_M) \\ &= f_{\hat{n}_1 \hat{n}_2 \ldots \hat{n}_M}(n_1, n_2, \ldots n_M) \cdot f_{\hat{\psi}_1 \hat{\psi}_2 \ldots \hat{\psi}_M}(\psi_1, \psi_2, \ldots, \psi_M) \\ &= \frac{1}{n_1} f_{\hat{n}_1}(n_1) f_{\hat{\psi}_1}(\psi_1) \cdots \frac{1}{n_M} f_{\hat{n}_M}(n_M) f_{\hat{\psi}_M}(\psi_M) \\ &= \prod_{i=1}^{M} \frac{f_{\hat{n}_i}(n_i)}{2\pi n_i} \ . \end{aligned} \tag{3.13}$$

Since the components of $\mathbf{n}_i$ are assumed to be identically-distributed, independent, Gaussian RVs, the pdf of $n_i = |\mathbf{n}_i|$ is Rayleigh distributed. The Rayleigh parameter is equal to the standard deviation of n_{ix} or n_{iy}, that is, $\sigma_{n_{ix}} = \sigma_{n_{iy}} = \sigma_i$, and

$$f_{\hat{n}_i} = \rho(\cdot, \sigma_i), \quad \text{for all } i. \tag{3.14}$$

It follows therefore that

$$f_{\hat{\mathbf{n}}_1 \hat{\mathbf{n}}_2 \ldots \hat{\mathbf{n}}_M}(\mathbf{n}_1, \mathbf{n}_2, \ldots, \mathbf{n}_M) = \prod_{i=1}^{M} \frac{\rho(n_i, \sigma_i)}{2\pi n_i} \ . \tag{3.15}$$

From the assumptions it follows that the multivariates $(\mathbf{s}_1, \ldots, \mathbf{s}_M)$ and $(\mathbf{n}_1, \ldots, \mathbf{n}_M)$ are independent. Consequently, the density function for their sum is given by the convolution of their multivariate densities,

$$f_{\hat{\mathbf{s}}_1 + \hat{\mathbf{n}}_1, \ldots, \hat{\mathbf{s}}_M + \hat{\mathbf{n}}_M} = f_{\hat{\mathbf{s}}_1, \ldots, \hat{\mathbf{s}}_M} * f_{\hat{\mathbf{n}}_1, \ldots, \hat{\mathbf{n}}_M} \ . \tag{3.16}$$

Using (3.13), (3.14), and the notation $\mathbf{v}_i = \mathbf{s}_i + \mathbf{n}_i$ and $v_i = |\mathbf{v}_i| = |\mathbf{s}_i + \mathbf{n}_i|$, an algebraic manipulation similar to that used in the 1-D case allows one to express (3.16) as

$$f_{\hat{\mathbf{v}}_1,\ldots,\hat{\mathbf{v}}_M}(\mathbf{v}_1,\ldots,\mathbf{v}_M) = \int_{\Re_+^M} d^M s \; f_{\hat{s}_1\ldots\hat{s}_M}(s_1,\ldots,s_M) \prod_{j=1}^{M} \frac{R(v_j,s_j,\sigma)}{2\pi v_j} \;, \tag{3.17}$$

where $\int_{\Re_+^M} d^M s \; = \int_0^\infty \cdots \int_0^\infty \; ds_1 \ldots ds_M$, $\Re_+ = [0,\infty)$, and where $\Re_+^M$ is the Mth Cartesian power of $\Re_+$.

If $\mathbf{v}_i$ is expressed in polar coordinates as $\mathbf{v}_i = (v_i \cos\chi_i, v_i \sin\chi_i)$, (3.17) can be written as

$$\begin{aligned} f_{\hat{\mathbf{v}}_1,\ldots,\hat{\mathbf{v}}_M}(\mathbf{v}_1,\ldots,\mathbf{v}_M) &= f_{\hat{\mathbf{v}}_1\ldots\hat{\mathbf{v}}_M}(v_1\cos\chi_1, v_1\sin\chi_1,\ldots,v_M\cos\chi_M, v_M\sin\chi_M) \\ &= \frac{1}{v_1\cdots v_M} f_{\hat{v}_1\ldots\hat{v}_M}(v_1,\ldots,v_M)\, f_{\hat{\chi}_1\ldots\hat{\chi}_M}(\chi_1,\ldots,\chi_M), \end{aligned} \tag{3.18}$$

where

$$f_{\hat{v}_1,\ldots,\hat{v}_M}(v_1,\ldots,v_M) = \int_{\Re_+^M} d^M s \; f_{\hat{s}_1\ldots\hat{s}_M}(s_1,\ldots,s_M) \prod_{j=1}^{M} R(v_j,s_j,\sigma) \;, \tag{3.19}$$

and

$$f_{\hat{\chi}_1\ldots\hat{\chi}_M}(\chi_1,\ldots,\chi_2) = \frac{1}{(2\pi)^M} \;. \tag{3.20}$$

Thus, under the specified assumptions, the radial and angular components of $(\mathbf{v}_1,\ldots,\mathbf{v}_M)$ are mutually independent and each angular component is uniformly distributed on $[0,2\pi)$.

The density of a sum of univariates $\hat{z} = \hat{v}_1 + \hat{v}_2 + \cdots + \hat{v}_M$ is determined by their joint density $f_{\hat{v}_1\hat{v}_2\ldots\hat{v}_M}(v_1,v_2,\ldots,v_M)$ according to

$$f_{\hat{z}}(z) = \int_{\Re_+^{M-1}} d^{M-1}w \; f_{\hat{v}_1\hat{v}_2\ldots\hat{v}_M}(w_1,w_2,\ldots,w_{M-1},z-w_1-w_2-\cdots-w_{M-1}) \;. \tag{3.21}$$

The expression (3.21) is the generalization of the well-known result[10] that, given two RVs $\hat{x}$ and $\hat{y}$ with joint pdf $f_{\hat{x}\hat{y}}(x,y)$, the pdf of their sum, $\hat{z} = \hat{x} + \hat{y}$, is given by

$$f_{\hat{z}}(z) = \int_{-\infty}^{\infty} f_{\hat{x}\hat{y}}(z-w,w) \; dw \;. \tag{3.22}$$

Thus (3.21) becomes the M-fold convolution of the 1-D marginal densities of the univariate RVs when the individual RVs are independent.

If (3.19) is introduced in (3.21) and the order of integration is changed, the M-dimensional integration in (3.21) will involve only the product of the Rice densities from (3.19), and will represent the convolution of these Rice functions. Formally, the result is

$$f_{\hat{z}}(z) = \int_{\Re_+^M} d^M s \; f_{\hat{s}_1\ldots\hat{s}_M}(s_1,\ldots,s_M) \; G(z,s_1,\ldots,s_M,\sigma) \;, \tag{3.23}$$

where

$$G(z, s_1, \ldots, s_n, \sigma) = [*_{i=1}^{M} R(\cdot, s_i, \sigma)](z) \ , \tag{3.24}$$

and where $*_{i=1}^{M}$ represents the M-fold convolution operator. Similarly to (2.21) for the 1-D case, (3.23) shows that the unconditional pdf, $f_{\hat{z}}(z)$, is the expected value of a conditional density function, namely the convolution of Rice functions given by (3.24). The conditional density function (3.24) is dependent on the constrained signal amplitudes, $(s_1, \ldots, s_M)$, that are distributed according to the multivariate pdf $f_{\hat{s}}(s)$.

The probability of detection follows from (3.6) and (3.23) as

$$P_d(b) = \int_{\Re_+^M} d^M s \ f_{\hat{s}_1 \ldots \hat{s}_M}(s_1, \ldots, s_M) \ P_d^R(b, s_1, \ldots, s_M, \sigma) \ , \tag{3.25}$$

where

$$P_d^R(b, s_1, \ldots, s_M, \sigma) = \int_b^\infty dz \ G(z, s_1, \ldots, s_M, \sigma) \ . \tag{3.26}$$

The expression (3.25) shows that, for a specified threshold, the probability of detecting a fluctuating target by summing M echos is the expected value of the constrained probability of detection of M "point targets" with the corresponding ensemble of "constant" target strengths distributed according to the multivariate pdf $f_{\hat{s}_1 \ldots \hat{s}_M}$.

The probability of false alarm can be derived from (3.25) by setting the signal components to zero. Thus the signal pdf is given by

$$f_{\hat{s}_1 \ldots \hat{s}_M}(s_1, \ldots, s_M) = \prod_{i=1}^{M} \delta(s_i) \ , \tag{3.27}$$

and this leads to

$$P_{fa}(b) = P_d^R(b, s_1 = 0, \ldots, s_M = 0, \sigma) = \int_b^\infty dz \ [*_{i=1}^{M} \rho(\cdot, \sigma)](z) \ , \tag{3.28}$$

where $\rho(r, \sigma)$ is the Rayleigh density (1.3). This could have been written directly, since the noise is assumed to be Rayleigh distributed and independent between echos. Together (3.25) and (3.28) constitute a parametric expression of the ROC curve.

The empirical estimate for the probability of detection follows from (3.25) if the pdf $f_{\hat{s}_1 \ldots \hat{s}_M}(s_1, \ldots, s_M)$ is replaced by the empirical multivariate pdf

$$f_{\hat{s}_1 \ldots \hat{s}_M}^E(s_1, \ldots, s_M) = \frac{1}{N} \sum_{k=1}^{N} \prod_{i=1}^{M} \delta(s_i - s_{ik}) \ . \tag{3.29}$$

The result is

$$P_d^E(b) = \frac{1}{N} \sum_{k=1}^{N} \int_b^\infty dz \ G(z, s_1, \ldots, s_M, \sigma) = \frac{1}{N} \sum_{k=1}^{N} P_d^R(b, s_{1k}, \ldots, s_{Mk}, \sigma) \ . \tag{3.30}$$

3.2 SPECIAL CASES

Formally simpler results can be obtained if the pdf for the sequence of signal amplitudes has a manageable analytical form. Such is the situation, for example, when the signal amplitudes are independent from ping-to-ping (random target aspect), when the signal amplitudes are identical ping-to-ping (no aspect change), or when the signal amplitude is constant.

3.2.1 Independent Signal Amplitudes Ping-to-Ping

Given empirical target strength data as a function of aspect, the independent echo case would correspond to a random change in aspect between echos. While this case is nonphysical, it is useful in checking the code developed to estimate the multiping ROC curves.

If the echos are independent, then the pdf for the ensemble of amplitudes is the product of the marginal pdfs,

$$f_{\hat{s}_1 \ldots \hat{s}_M}(s_1, \ldots, s_M) = f_{\hat{s}_1}(s_1)\ f_{\hat{s}_2}(s_2) \cdots f_{\hat{s}_M}(s_M)\ , \tag{3.31}$$

and (3.19) can be written as

$$f_{\hat{v}_1,\ldots,\hat{v}_M}(v_1, \ldots, v_M) = \prod_{i=1}^{M} \int_0^\infty ds_i\ f_{\hat{s}_i}(s_i)\ R(v_i, s_i, \sigma)\ . \tag{3.32}$$

If this expression for $f_{\hat{v}_1,\ldots,\hat{v}_M}(v_1, \ldots, v_M)$ is introduced in (3.21), it follows that the pdf for the sum of amplitudes is the convolution of M identical replicas of the univariate pdf for the amplitude of one echo given by (2.21), i.e.,

$$f_{\hat{z}}(z) = [*_{i=1}^{M} f_{|\hat{\mathbf{s}}+\hat{\mathbf{n}}|}](z)\ . \tag{3.33}$$

This expression could have been written immediately, based on the independence of the signal and noise components.

The empirical estimate of $f_{\hat{z}}(z)$ follows from (3.46) if $f_{|\hat{\mathbf{s}}+\hat{\mathbf{n}}|}(z)$ is replaced by its empirical estimate

$$f^E_{|\hat{\mathbf{s}}+\hat{\mathbf{n}}|}(z) = \frac{1}{N} \sum_{i=1}^{N} R(z, s_i, \sigma)\ , \tag{3.34}$$

obtained from (2.21) and (2.27). The empirical probability of detection can now be estimated numerically by using (3.34), (3.33), and (3.6).

3.2.2 Identical Signal Amplitudes Ping-to-Ping

If the observed target strength (signal amplitude) is constant for any set of M successive pings, then the pdf of the M-variate signal is

$$f_{\hat{s}_1 \ldots \hat{s}_M}(s_1, \ldots, s_M) = f_{\hat{s}_1}(s_1)\ \delta(s_2 - s_1) \cdots \delta(s_M - s_1)\ . \tag{3.35}$$

If (3.35) is used in (3.19), the result is

$$f_{\hat{v}_1\hat{v}_2\ldots\hat{v}_M}(v_1, v_2, \ldots, v_M) = \int_0^\infty ds\, f_{\hat{s}}(s) \prod_{i=1}^{M} R(v_i, s, \sigma) \ , \tag{3.36}$$

where R is the Rice function (1.4) and s_1 is simply denoted by s. If (3.36) is introduced in (3.21) and the order of integration is changed, the result is

$$f_{\hat{z}}(z) = \int_0^\infty ds\ f_{\hat{s}}(s)\ G(z, s, \sigma) \ , \tag{3.37}$$

where $G(z, s, \sigma)$ is the convolution of P identical replicas of the Rayleigh-Rice pdf with respect to the first dependent variable, i.e.,

$$G(z, s, \sigma) = [*_{i=1}^{M} R(\cdot, s, \sigma)](z) \ . \tag{3.38}$$

Recalling that $\hat{z} = \hat{v}_1 + \hat{v}_2 + \cdots + \hat{v}_M$, the probability of detection follows from (3.6) with (3.37) and (3.38) as

$$\begin{aligned} P_d(b) &= \int_b^\infty dr \int_0^\infty ds\ f_{\hat{s}}(s)\ G(r, s, \sigma) \\ &= \int_0^\infty ds\ f_{\hat{s}}(s) \int_b^\infty dr\ G(r, s, \sigma) \\ &= \int_0^\infty ds\ f_{\hat{s}}(s) P_d^R(b, s, \sigma) \ . \end{aligned} \tag{3.39}$$

The expression $P_d^R(b, s, \sigma) = \int_b^\infty dr\ G(r, s, \sigma)$ is the single-ping version of (3.26) and has been tabulated by Robertson.[11] This special case corresponds to a random (unknown) aspect target, but where the aspect remains fixed over any given set of M pings (observations). Expression (3.39) shows that the probability of detection (P_d) for this special case is given by a weighted average of the P_d for M constant amplitude signals where the weighting is defined by the pdf of the signal amplitudes, $f_{\hat{s}}(s)$.

The empirical estimate for the probability of detection is obtained by replacing the pdf of s in (3.39) with its empirical estimate,

$$f_{\hat{s}}^E(s) = \frac{1}{N} \sum_{k=1}^{N} \delta(s - s_k) \ . \tag{3.40}$$

Here $\{s_k\}_{k=1}^N$ corresponds to the set of target strength values (signal amplitudes) measured for a uniformly distributed (equally likely) set of aspect angles. The result is

$$P_d(b) = \frac{1}{N} \sum_{k=1}^{N} P_d^R(b, s_k, \sigma) \ . \tag{3.41}$$

3.2.3 Constant Amplitude Signals

If the signal amplitude for each ping, A_i, is a constant, A, then

$$f_{\hat{s}_1 \ldots \hat{s}_M}(s_1, \ldots, s_M) = \delta(s_1 - A) \cdots \delta(s_M - A) \ . \tag{3.42}$$

With (3.42), (3.19) becomes

$$f_{\hat{v}_1,\ldots,\hat{v}_M}(v_1, \ldots, v_M) = \prod_{i=1}^{M} R(v_i, A, \sigma) \ , \tag{3.43}$$

and (3.21) reduces to

$$f_{\hat{z}}(z) = [*_{i=1}^{M} R(\cdot, A, \sigma)](z) \ . \tag{3.44}$$

This could have been obtained from (3.38) by making

$$f_{\hat{s}}(s) = \delta(s - A). \tag{3.45}$$

Substituting (3.44) into (3.6), the resulting probability of detection is

$$P_d^R(b) = \int_b^\infty dz \ [*_{i=1}^{M} R(\cdot, A, \sigma)](z) \ . \tag{3.46}$$

The ROC curves derived from (3.46) and the corresponding P_{fa} (3.28) were charted by Robertson.[11]

This page intentionally left blank.

4. NUMERICAL EXAMPLES

This section provides selected examples of ROC computations to illustrate the analytical development presented in the preceding sections. Equations (3.25) and (3.28) allow straightforward numerical computation of linear detector ROC curves for analytical pdfs as well as for empirical data.

For the case of a constant target (constant signal amplitude) and independent, Gaussian noise, the P_d can be computed by convolving the Rician pdf for the desired SNR with itself M-1 times, where M is the number of pings to be integrated [see (3.46)]. The corresponding P_{fa} is given by (3.28). Example ROC curves for the constant signal case are shown in Figure 4.1 for SNR = 9 dB and for the integration of 1, 2, and 4 echoes.

The numerical computations for the case of a constant amplitude target were validated through comparisons with equivalent results published by Robertson[11,12] for selected test cases. The P_d values, for a given P_{fa} and SNR, computed using the methods developed here, differed from the corresponding P_d values given by Robertson by less than 1%. Equivalently, the small differences observed in the P_d values correspond to a difference of less than 0.05 dB in the SNR required to achieve a specified P_d and P_{fa}.

ROC curves for a Rayleigh-fluctuating target in Gaussian noise are shown in Figure 4.2. The signal amplitudes are assumed to be independent from ping-to-ping. Curves are shown for 1-, 2-, and 4-ping integration and an average SNR of 9 dB. The average SNR is defined as $\alpha^2/2\sigma^2$, where α is the Rayleigh distribution parameter and σ is the standard deviation of the Gaussian noise. The pdf of the multiping detection statistic in (3.23) is obtained by computing the normalized sum of Rayleigh-weighted Ricians for the single-ping case (2.21) and then convolving the resulting pdf with itself the appropriate number of times.

The numerical computations for the Rayleigh-fluctuating target ROC curves were validated through comparison with the closed-form solution for the single-ping case, eqs. (2.35) and (2.36), and with the results of a Monte Carlo simulation for the multiping case. The reduction in performance (lower P_d for a given P_{fa}) for a Rayleigh-fluctuating target with average SNR = 9 dB, relative to the performance for a constant target with SNR = 9 dB, is evident from comparison of Figure 4.2 with Figure 4.1.

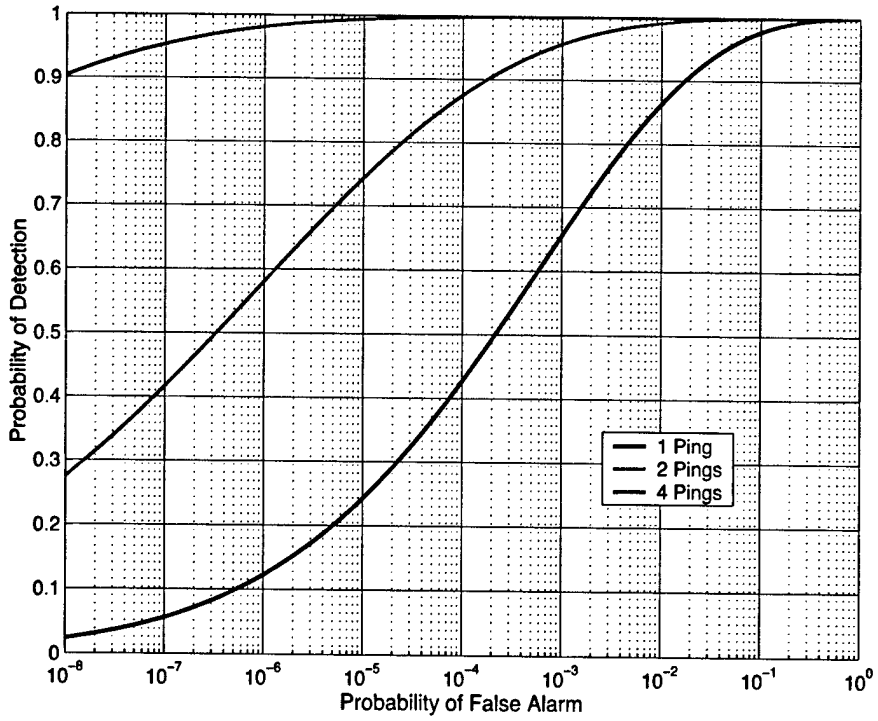

Figure 4.1 Example ROC curves for a constant amplitude target. SNR = 9 dB; 1-, 2-, 4-ping integration

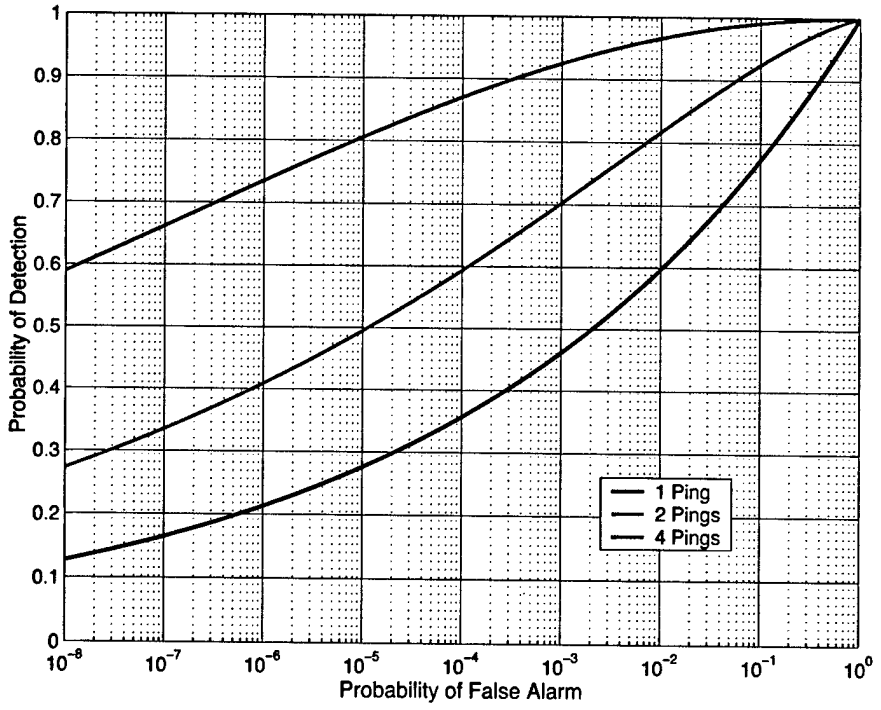

Figure 4.2 Example ROC curves for a Rayleigh-fluctuating target. Avg. SNR = 9 dB; 1-, 2-, 4-ping integration

Now consider the estimation of detector performance for two actual targets, referred to here as target A and target B. Figures 4.3 and 4.4 compare the measured target strength values for the two targets. Figure 4.3 shows the polar scattering patterns (relative target strength as a function of target aspect angle), while Fig. 4.4 shows the cumulative distribution functions (cdfs) of the target strength values over all aspect angles. As seen from Fig. 4.3, the target strength of target A is larger than that of target B for most aspect angles. In Fig. 4.4, the cdf for target B has been shifted by approximately +7 dB relative to the cdf for target A in order to make the average SNR values equal for the two targets. The target strength characteristics for these two targets are clearly very different.

Figure 4.5 illustrates how the expected detection performance over all aspects, i.e., the expected detection performance for a random aspect encounter with the target, depends on the target strength characteristics of these two targets. ROC curves, computed using (3.28) and (3.30), are shown for both single-ping detection and for the integration of four pings. The target strength values and noise statistics were scaled so that the average SNR was 9 dB for both targets, where the average SNR is defined by Eq. (3.9). Thus, the differences between the ROC curves for targets A and B result from the differences in the shapes of the target strength cdfs (Fig. 4.4) rather than from absolute differences in the target strength values (Fig. 4.3) for these two targets.

In many applications, detection performance against a particular target is computed based on a point target representation; i.e., a single target strength value is used to represent the (statistical) encounter with the target. A common approach is to use an order statistic, from the target strength versus aspect values, that corresponds to the desired probability of detection. For example, if a 90% probability of detection is desired, the lower 10th percentile target strength value is used to represent the target. The objective of this procedure is to force a conservative estimate of performance prediction relative to the actual performance.

Figure 4.6 compares the ROC curve for target B, computed using the methods of this paper that incorporate the target strength measurements for all aspects, with ROC curves for a point target (constant signal amplitude) assumption. The blue curve shows the estimated ROC curve for target B for 4-ping integration and an average SNR of 10.8 dB. The red curves are the corresponding 4-ping ROC curves for the constant (point) target assumption at SNRs equivalent to the 10th (lower curve) and 50th (upper curve) percentile values of the target strength distribution for target B. The lower 10th percentile corresponds to an SNR of 2.5 dB while the 50th percentile SNR is 7.0 dB. Clearly, the ROC curves for the point target assumption provide a poor representation of the expected detection performance for this target.

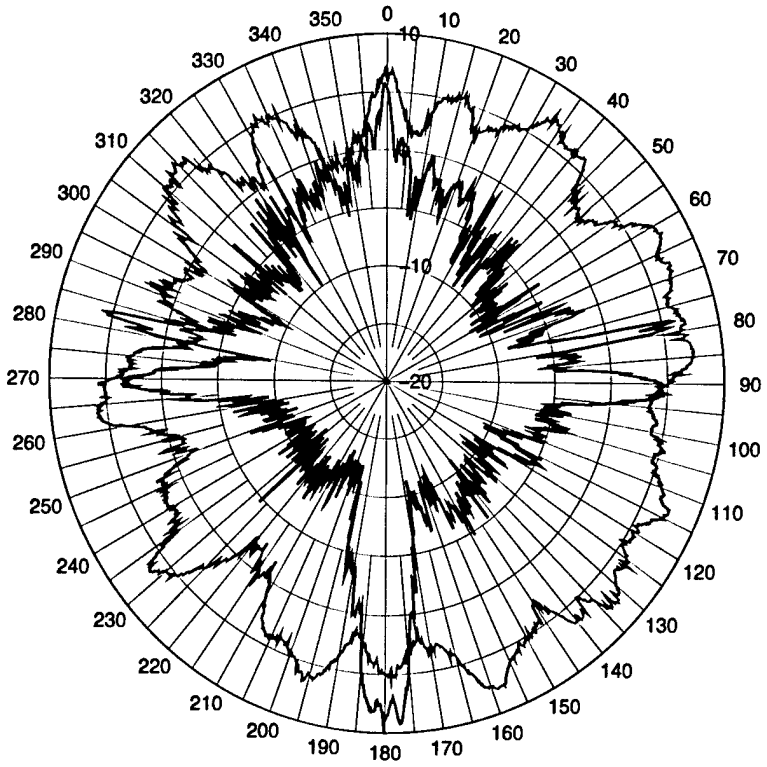

Figure 4.3 Relative target strength (dB) versus aspect for two mine targets; target A (red), target B (blue)

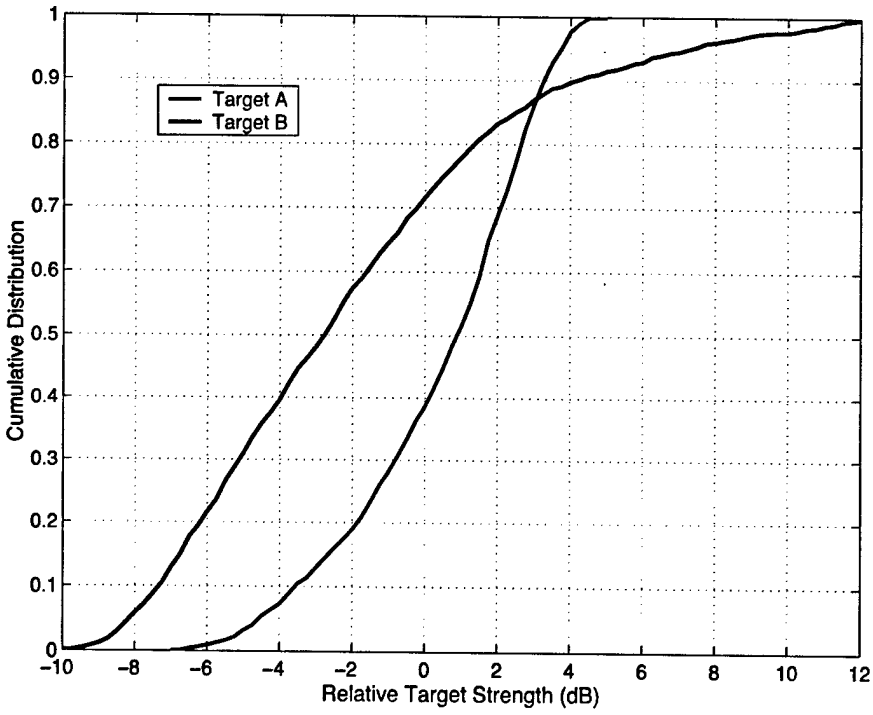

Figure 4.4 Cumulative distribution of target strength values; target A (red), target B (blue)

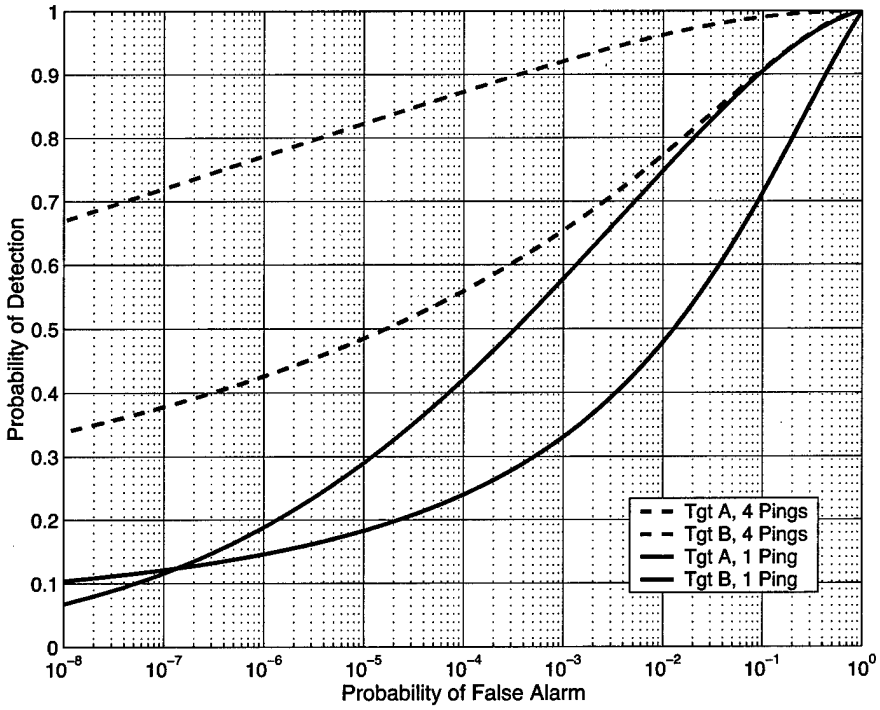

Figure 4.5 ROC curve comparison for targets A (red) and B (blue). Avg. SNR = 9 dB; 1-, 4-ping integration

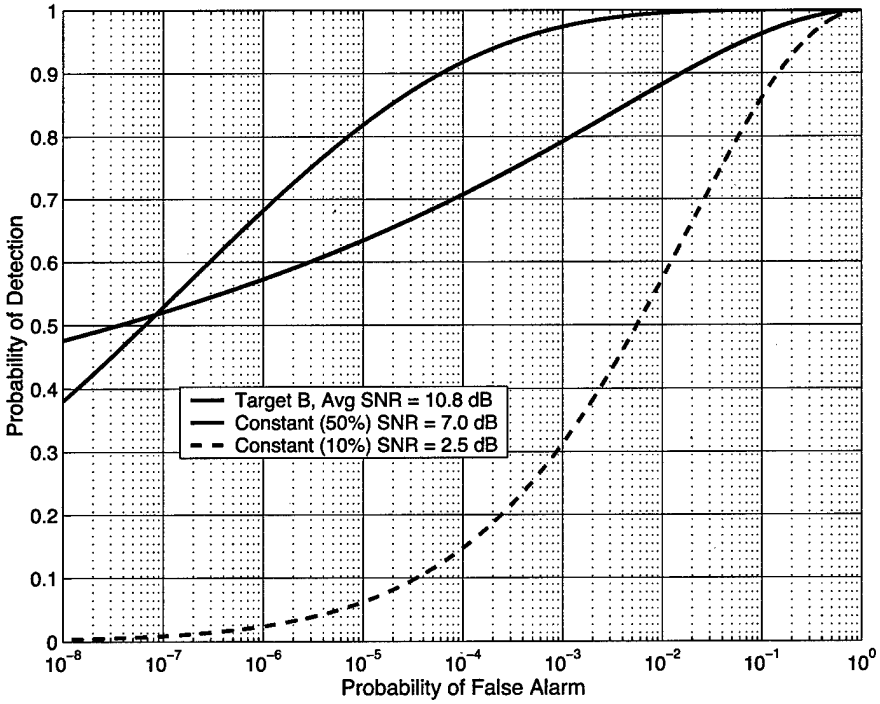

Figure 4.6 ROC curve comparison for target B (blue) with constant-signal point targets (red)

Figure 4.7 shows a set of ROC curves for target B for the case of 2-ping integration for average SNRs of 6, 9, 12, 15, and 18 dB. Figure 4.8 shows a similar set of ROC curves for target B with an average SNR of 9 dB where the number of pings integrated varies from 1 to 16 pings. While these curves assume a random target aspect for the encounter (all aspects are equally likely), it is straightforward to include any *a priori* knowledge about the target aspect or range of target aspects in the ROC curve computations.

The ROC curves in the previous figures show the expected multiping detection performance when all target aspects are equally likely and when the aspect is constant over any given set of multiping observations. The effect of ping-to-ping changes in aspect on detection performance is illustrated in Fig. 4.9. ROC curves are shown for target B for an average SNR of 9 dB with 8 pings integrated for a fixed aspect (no aspect change), a shift in the observed aspect of 0.4 degrees per ping, and a shift of 2.0 degrees per ping. In addition, the ROC curve is shown for the case of a random aspect shift from ping to ping. As in the previous figures, the ROC curves represent the expected performance for a random aspect encounter with the target. The independent aspect case represents an approximate upper bound on performance for ping-to-ping aspect changes typical of a real-world encounter.

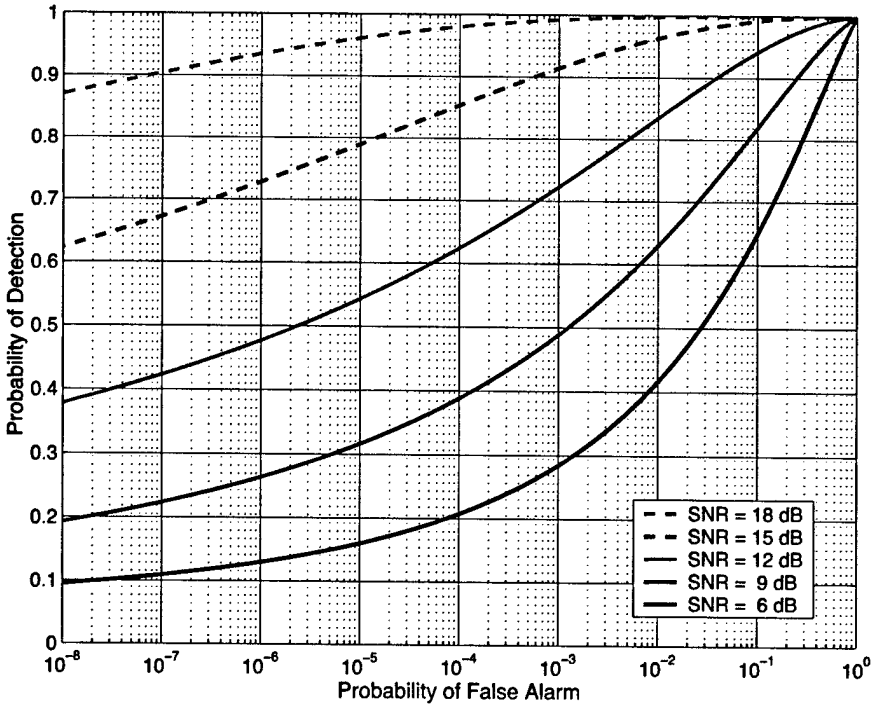

Figure 4.7 Target B ROC curves versus SNR.
2-ping integration; Avg. SNR = 6, 9, 12, 15, 18 dB

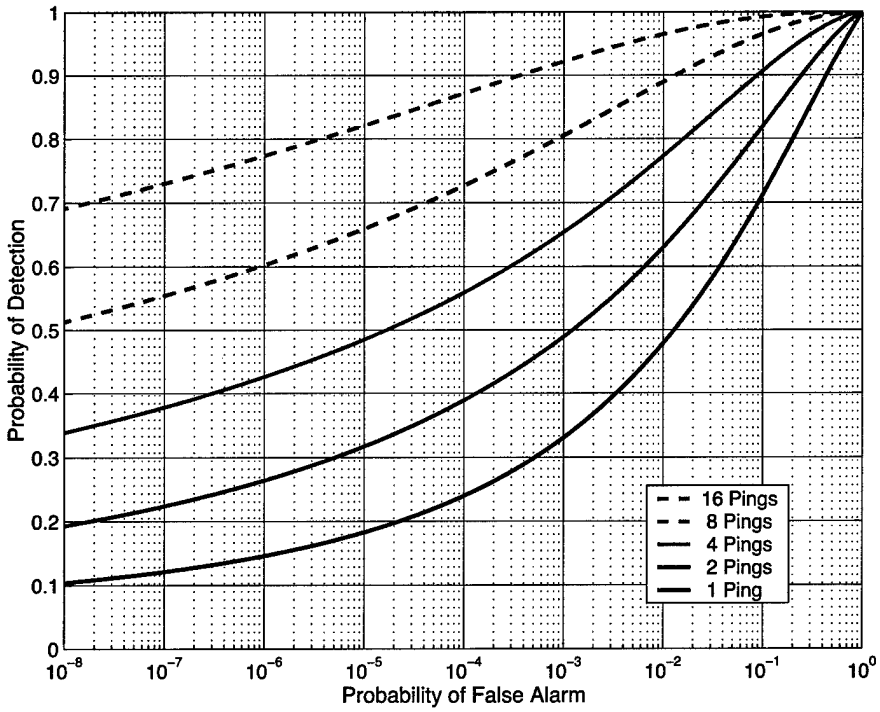

Figure 4.8 Target B ROC curves versus number of pings. Avg. SNR = 9 dB; 1-, 2-, 4-, 8-, 16-ping integration

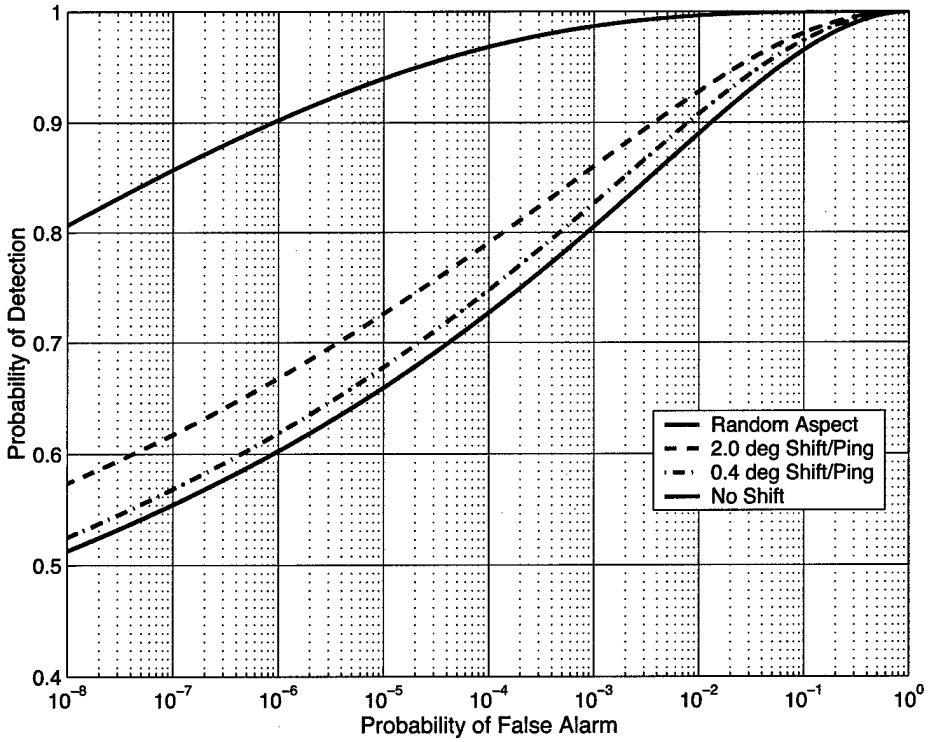

Figure 4.9 Target B ROC curves – effects of ping-to-ping aspect shift. Avg. SNR = 9 dB; 8-ping integration

This page intentionally left blank.

5. SUMMARY

This work presents a method for incorporating target scattering patterns directly into the computation of statistical detection performance for a linear detector followed by a post-detector integrator that sums the detected peaks over multiple echoes. Target scattering patterns (e.g., acoustic target strength or radar cross-section) characterize the echo-to-echo fluctuations in level due to changes in observed target aspect. In this work, the scattering patterns of interest are obtained from direct measurement of acoustic target strength of underwater bottom mines; however, scattering patterns obtained from theoretical models or other means can be used as well.

As illustrated by the examples in the previous section, the methodology presented here supports estimation of multi-ping Receiver Operating Characteristic (ROC) curve performance for any simulation scenario of interest. For example, detection performance can be estimated for a random encounter with a specific target (i.e., initial aspect unknown), for a specific sonar-target encounter geometry as a function of the initial observed target aspect, or as a function of the range of target aspects observed in a sonar-target encounter. Alternatively, the method can be used when the received signal amplitudes are described by an analytic distribution. The methodology can be extended to the general detector-averager problem for sampled time-varying echo envelopes given that successive samples of the received signal-plus-noise are independent.

REFERENCES

1. Marcum, J. I., "A Statistical Theory of Target Detection by Pulsed Radar," The RAND Corp., Res. Memo. RM-754; 1 December 1947; also published in IEEE Trans. Info. Theory, vol. IT-6, no. 2, pp. 59-144 (April 1960).

2. Marcum, J. I., "Mathematical Apendix," The RAND Cor., Res. Memo. RM-753; 1 July 1948; also published in IEEE Trans. Info. Theory, vol. IT-6, no. 2, pp. 145-267 (April 1960).

3. Swerling, P., "Probability of Detection for Fluctuating Targets," The Rand Corp., Res. Memo. RM-1217; 17 March 1954.

4. Swerling, P., "Detection of Fluctuation Pulse Signals in the Presence of Noise," IRE Trans. Info. Theory, pp. 175-178 (September 1957).

5. Kaplan, E. L., "Signal Detection Studies, with Applications," Bell Sys. Tech. J., vol. 34, (March 1955).

6. Schwartz, M., "Effects of Signal Fluctuation in the Detection of Pulsed Signals in Noise," IRE Trans Info. Theory, vol. IT-2, pp. 66-71 (June 1956).

7. Swerling, P., "Radar Probability of Detection for Some Additional Fluctuating Targets," IEEE Trans. Aerospace Electron. Syst., vol. 33, no. 2, pp. 698-709 (April 1997).

9. Abramovitz, M. and I. A. Stegun, *Handbook of Mathematical Functions* (Dover Publications Inc., New York), Dec. 1972.

10. Papoulis, A., *Probability and Statistics* (Prentice Hall Inc., Englewood Cliffs), 1990.

11. Robertson, G. H., "Operating Characteristics for a Linear Detector of CW Signals in Narrow-Band Gaussian Noise," The Bell System Technical Journal, pp. 755-774 (April 1967).

12. Tufts, D. W. and A. J. Cann, "On Albersheim's Detection Equation," IEEE Trans. Aerospace Electron. Syst., vol. 19, no. 4, pp. 643-646 (July 1983).

This page intentionally left blank.

Copy No.

14 March 2003

DISTRIBUTION LIST FOR ARL-TR-02-03 Technical Report under Contract N00039-96-D-0051 TD No. 250605, Multiple-Ping Processing for Detection of Targets on the Sea Bottom

Copy No.

Office of Naval Research
Ballston Center Tower One
800 N. Quincy Street
Arlington, VA 22217-5660

1 Attn: Dr. Doug Todoroff, Code 32CM
2 Dr. John Tague, Code 321US
3 Mr. Dave Armstrong, Code 321US

Coastal Systems Station
6703 W. Highway 98
Panama City, FL 32407-7001

4 Attn: Dr. John Lathrop
5 Sam Richardson

6 Bruce Johnson
NAVEODTECHDIV
2008 Stump Neck Road
Indian Head, MD 20640

7 Sudha Reese, Code 311
Naval Undersea Warfare Center
1176 Howell Street
Newport, RI 02841

Defense Technical Information Center
8725 John J. Kingman Rd., Suite 0944
Fort Belvoir, VA 22060-6218

8-10 Attn: DTIC-OCC

Applied Research Laboratory
Pennsylvania State University
P. O. Box 30
State College, PA 16801

11 Attn: Dr. Doug Abraham
12 Frank Symons

Copy No.

McKinney Engineering Library
ECJ 1.300
Austin, TX 78712
13 Attn: Librarian

14-16 Petre Rusu
J3S, Inc.
11921 N. Mopac Expressway, Suite 360
Austin, TX 78759-3556

17 R. S. Bailey, ARL:UT

18 M.-F. Chang, ARL:UT

19 K. B. Fisher, ARL:UT

20 T. L. Henderson, ARL:UT

21 J. M. Huckabay, ARL:UT

22 C. M. Loeffler, ARL:UT

23 S. K. Mitchell, ARL:UT

24 C. S. Penrod, ARL:UT

25–34 S. P. Pitt, ARL:UT

35 T. D. Plemons, ARL:UT

36 M. B. Revesz, ARL:UT

37 K. N. Scarbrough, ARL:UT

38 G. R. Wilson, ARL:UT

39 Library, ARL:UT